Journal of Environmental Chemical Engineering 10 (2022) 107854

Contents lists available at ScienceDirect

Journal of Environmental Chemical Engineering

journal homepage: www.elsevier.com/locate/jece

Comparison of UV, chlorination, UV-hydrogen peroxide and UV-chlorine processes for tramadol removal: Kinetics study and transformation products identification

M. Cobo-Golpe, V. Fernández-Fernández, T. Arias, M. Ramil, R. Cela, I. Rodríguez *

Department of Analytical Chemistry, Nutrition and Food Sciences, Research Institute on Chemical and Biological Analysis (IAQBUS), Universidade de Santiago de Compostela, 15782 Santiago de Compostela, Spain

ARTICLE INFO

Editor: Xin Yang

Keywords:
Tramadol
Oxidative processes
Liquid chromatography mass spectrometry
Removal efficiency
Transformation products

ABSTRACT

Tramadol (TRA) is a poorly biodegradable pharmaceutical, ubiquitously distributed in the aquatic environment. Herein, we present a thorough comparison of two conventional (UV and chlorination) and two advanced oxidative processes (UV-H_2O_2 and UV-chlorine), in terms of TRA removal efficiency and transformation products (TPs) formation. The performance of these processes was evaluated in different complexity water samples, previously adjusted at neutral pH. Using 1 mg L^{-1} as initial concentration of oxidant, UV-chlorine was the most effective process followed by UV-H_2O_2, direct photolysis and chlorination. The efficiency of the investigated treatments decreased for surface and wastewater samples compared to model solutions. Despite this limitation, the UV-chlorine treatment removed more than 70% of TRA measured in wastewater samples after 5 min of UV irradiation, in presence of 10 mg L^{-1} of chlorine. UV-chlorine involved additional degradation routes to those described for the rest of treatments, including the formation of tramadol-N-oxide, several chlorinated derivatives, and the volatile species chloroform, 1,1-dichloroacetone and anisole. Some of these specific TPs might pose a similar toxicity to that associated to the parent compound; however, their maximum formation yields remained below 2.5%, decreasing steady for reaction times longer than 5 min

1. Introduction

Tramadol (TRA) is a pharmaceutical prescribed for the treatment of pain. The parent drug and several human metabolites (i.e. N-desmethyl and O-desmethyl forms) are excreted through urine ending at urban sewage treatment plants (STPs) [1,2]. The low removal efficiency of TRA during biological treatments employed in these facilities (from activated sludge to bio-filtration) [3–5] leads to the discharge of this compound in the aquatic environment. Concentrations reported in this compartment range from the low ng mL^{-1} to dozens of ng L^{-1} in treated wastewater and surface water samples, respectively [5,6]. More specifically, Gurke and co-workers [3] reported a median level of 0.68 ng mL^{-1} for TRA during a 10-days sampling campaign of the effluent stream from the same STP. Average concentrations reported by other authors in the same matrix were in the range of 20 ng mL^{-1} [5,6]. TRA has been also noticed in soils, sediments and wetlands affected by sewage water discharges [7]; moreover, it shows limited attenuation during riverbank filtration of polluted waters [8]. To sum up, TRA is recognized as a persistent, relatively polar (log D −0.06 at pH 7) and mobile pollutant in the water phase.

In order to limit the discharges of TRA to the aquatic environment, several oxidative treatments are under evaluation. In spiked model solutions, TRA reacts with free chlorine with formation of N-desmethyl and carbonyl transformation products (TPs), a range of chlorinated derivatives with a close structure to that of the parent drug, and breakdown compounds generated through hydrolysis of the bond between cyclohexane and anisole rings [9]. Formation of hydroxylated and chlorinated derivatives has been also reported during UV irradiation of spiked water samples in presence of H_2O_2, using monochloramine as a source of chlorine [10]. As regards wastewater samples, the possibility to reduce the concentrations of TRA existing in this matrix has been proved using different sources of UV light, either employed alone [11] or combined with H_2O_2 in advanced oxidative processes (AOPs) [12,13]. Ozonization has been tested in pilot scale facilities [14]. In this study, authors highlighted the formation of N-oxide, as a concerning TP of TRA in wastewater. Same derivative was also noticed during photocatalytic

* Corresponding author.
E-mail address: isaac.rodriguez@usc.es (I. Rodríguez).

https://doi.org/10.1016/j.jece.2022.107854
Received 21 February 2022; Received in revised form 22 April 2022; Accepted 2 May 2022
Available online 5 May 2022

treatment of spiked water samples in presence of TiO_2 particles [15].

Despite these previous studies, a thorough comparison of the kinetics of TRA dissipation, its reaction routes and the generated TPs, when different oxidative treatments are applied to aliquots of the same water matrix, is missed. Moreover, to the best of our knowledge, the combination of UV irradiation and free chlorine ($HClO/ClO^-$) has not been evaluated for the removal of TRA, despite the fact that its efficiency has been demonstrated previously for other poorly biodegradable pharmaceuticals [16]. In addition to hydroxyl radicals ($HO^{\cdot}$), the photodecomposition of free chlorine generates a series of reactive chlorine species (RCS), with the chlorine radical ($Cl^{\cdot}$) being the most abundant one, and also that formed directly from free chlorine photodecomposition [17,18], Eq. (1). Both radicals ($HO^{\cdot}$ and $Cl^{\cdot}$) show high redox potentials and present complementary reactivity towards organic compounds; thus, the photochemical decomposition of free chlorine (Eqs. (1, 2)) might be more effective than the combined use of UV radiation and H_2O_2, which renders just $HO^{\cdot}$, Eq. (3). Moreover, at 254 nm, the molar extinction coefficient of free chlorine is about three times higher than that of H_2O_2 [18].

$$ClOH/ClO^- + UV\ (254\ nm) \rightarrow HO^{\cdot}/O^{\cdot-} + Cl \quad (1)$$

$$O^{\cdot-} + H_2O \rightarrow HO^{\cdot} + HO^- \quad (2)$$

$$H_2O_2 + UV\ (254\ nm) \rightarrow 2\ HO \quad (3)$$

Herein, we compare the efficiency of direct photolysis (using 254 nm light), chlorination ($HClO/ClO^-$), and the AOPs UV-H_2O_2, and UV-chlorine for the removal of TRA, reporting the suite of TPs generated during each treatment and their time-course stability. Procedures showing the best performance in model solutions were further evaluated with environmental samples of river and wastewater. The evolution of TRA during above treatments was followed by injection of water samples aliquots in a liquid chromatography (LC) quadrupole time-of-flight (QTOF) mass spectrometry (MS) system. Furthermore, gas chromatography (GC) TOF-MS was considered to assess the formation of volatile derivatives not amenable to electrospray (ESI) ionization.

2. Material and methods

2.1. Solvents, standards and samples

Methanol (MeOH), HPLC-grade purity, formic acid (FA, 98%) and pentane, trace analysis grade, were acquired from Merck (Darmstadt, Germany). Ultrapure deionized water (18.2 MΩ cm^{-1}) was obtained from a Geni U system (Rephile, Shanghai, China). Potassium phosphate salts (K_2HPO_4 and KH_2PO_4), ascorbic acid, potassium iodide, sodium sulfate, sodium bicarbonate, sodium chloride, sodium nitrate, H_2O_2, and sodium hypochlorite (6–14%) were provided by Sigma-Aldrich (Milwaukee, WI, USA). The exact concentration of the two later reagents were determined by titration, with standardized solutions of potassium permanganate and sodium thiosulfate (in presence of an excess of potassium iodide) for H_2O_2 and free chlorine analysis, respectively. Diluted solutions of sodium hypochlorite were prepared in ultrapure water and maintained at 4 ºC for a maximum of 5 days. Before use, their concentrations were verified by reaction with N,N-diethyl-p-phenylenediamine with photometric detection [19].

TRA, its isotopically enriched analog (labeled in the methoxy moiety, TRA-^{13}C-d_3, 100 μg mL^{-1} in MeOH), tramadol-N-oxide and N-desmethyl tramadol, nitrobenzene (NB) and p-chlorobenzoic acid (CBA) were purchased from Sigma-Aldrich. Individual standards of these compounds were prepared in MeOH. Standards of anisole, 1,2-dibromopropane (1,2-DBP), a mixture of trihalomethanes and other volatile disinfection by-products (DBPs) were obtained from Sigma-Aldrich and Dr. Ehrenstorfer (Augsburg, Germany), Table S1. Diluted mixtures of volatile halogenated compounds (containing trihalomethanes and other DBPs) and anisole were prepared in MeOH and pentane.

Surface and treated wastewater samples were obtained from a local river, and two STPs equipped with primary and activated sludge treatments. Samples were filtered (using glass fiber and cellulose acetate 0.45 μm pore size filters) before being employed in degradation studies. Table S2 compiles some characteristics of these samples.

2.2. TRA oxidative treatments

Assays aiming for the removal of TRA were performed using different water samples. In a first series of experiments, TRA was added to model solutions of ultrapure water (previously buffered at pH 7) at concentrations of 0.005 and 0.5 mg L^{-1}, during investigation of its degradation rate and identification of potential TPs, respectively. The initial concentration of TRA employed during assessment of its degradation rate was within the range of values reported for this pollutant in treated wastewater samples [3,5,6]. Additional assays were carried out with spiked river water (0.005 mg L^{-1}) and non-spiked wastewater samples. The initial concentrations of oxidants varied between 1 and 10 mg L^{-1}, depending on the employed compound (H_2O_2 or free chlorine), the purpose of the assay (kinetics study or TPs identification), and the initial concentration of TRA.

Photodegradation experiments were carried out in a home-made UV reactor housing an 8 W low pressure mercury lamp (Philips reference G8T5), emitting at 254 nm and assembled orthogonally to a cylindrical quartz reaction vessel (200 mm length x 32 mm o.d., Afora, Barcelona, Spain), containing 25 mL of the considered water sample. The fluence of radiation on the water sample (1.04 $\times 10^{-6}$ Einstein L^{-1} s^{-1}) was experimentally determined using potassium iodide as chemical actinometer.

Spiked water samples were prepared directly in the photoreaction vessels. First, a small volume (10–100 μL) of a TRA standard in MeOH was disposed in the quartz tube. The organic solvent was evaporated at room temperature, using a gentle stream of nitrogen, and TRA was redissolved with the considered water matrix (25 mL), previously buffered at pH 7 by addition of 1 mL of a 0.3 M solution of K_2HPO_4/KH_2PO_4. Thereafter, vessels were either exposed to UV light (direct photolysis experiments), or spiked with the considered oxidant (free chlorine or H_2O_2). Zero time aliquots were taken before inserting the vessel in the photoreactor (case of AOPs), before addition of oxidant (chlorine or H_2O_2), or before UV irradiation (direct photolysis). Control experiments were prepared in absence of UV light and/or oxidant. Free chlorine oxidation experiments were carried out in same reaction vessels, not exposed to UV light.

Water aliquots (0.5 mL) were withdrawn at increasing reaction times and transferred to amber vessels containing 0.05 mL of a standard solution of TRA-^{13}C-d_3 in methanol, and 10 μL of ascorbic acid (60 mg L^{-1} in ultrapure water). Methanol served as quencher of radical species generated during AOPs [17], whilst ascorbic acid neutralized the excess of oxidant (H_2O_2 or chlorine) [20]. Concentrations of H_2O_2 and free chlorine during the time-course of AOPs experiments were controlled using colorimetric reactive strips (obtained from Sigma-Aldrich) and photometric detection, respectively [19], before quenching the oxidant with ascorbic acid. For the determination of the total organic carbon (TOC) content of treated samples following AOPs, the excess of oxidant was removed by addition of 0.25 mL of a 60 mg mL^{-1} solution of sodium thiosulphate and no methanol was added. TOC was determined using non-dispersive infrared spectroscopy, after acidification of treated water samples and CO_2 purge, followed by oxidation of organic matter.

Time-course of TRA, and formation of TPs closely related with the chemical structure of the parent compound, were measured by injection of different reaction times aliquots in a LC-QTOF-MS instrument. The ratio between peak areas for the $[M+H]^+$ ions of TRA (264.1963) and TRA-^{13}C-d_3 (268.2182, both extracted with a mass window of 10 ppm) were compared to those obtained for calibration standards of TRA in ultrapure water (0.05–100 μg L^{-1}). The $[M-H]^-$ ion used to follow the evolution of CBA in competitive kinetics was that at m/z 154.9900. The

Table 1
Observed reaction rate constants (k, min^{-1}), half-lives ($t_{1/2}$, min) and determination coefficients (R^2) for the natural logarithmic plots of TRA normalized concentrations versus reaction time in spiked (0.005 mg L^{-1}) ultrapure water solutions buffered at pH 7.

Treatment	Constant	Value (min^{-1})	$t_{½}$ (min^{-1})	R^2
Chlorine (1 mg L^{-1})	$k_{TRA\text{-}chlorine}$	0.0219	31.7	0.994
UV (254 nm)	$k_{TRA\text{-}UV}$	0.0475	14.4	0.990
UV-H_2O_2 (1 mg L^{-1})	$k_{obsTRA\text{-}UV\text{-}H2O2}$	0.2005	3.52	0.996
UV- chlorine (1 mg L^{-1})	$k_{obsTRA\text{-}UV\text{-}chlorine}$	0.3785	1.83	0.989

time-course of NB was followed by LC with UV detection, under conditions provided in the experimental section, Text S1.

In order to investigate the formation of volatile halogenated species, treated water samples were processed using a variation of EPA 551.1, LLE extraction method [21] (US-EPA 1995a). In brief, 5 mL aliquots were transferred to a 10 mL vessel and spiked with 1,2-DBP (as IS). After addition of 1 mL of n-pentane and 3.5 g of sodium sulfate, vessels were closed and shaken manually for 5 min. The organic layer was recovered and analyzed by GC-TOF-MS. Calibration standard solutions (5–500 μg L^{-1}) were prepared dissolving the commercial mixture of trihalomethanes, and other volatile DBPs in pentane. Detailed GC-TOF-MS determination conditions are given as supplementary information, Text S2, Table S1.

2.3. Equipment

The dissipation of TRA through the series of oxidative processes considered in this research, and the identification of most TPs were carried out using a UPLC-QTOF-MS instrument: Agilent 6550 model, furnished with an electrospray ionization source (ESI), and combined with a 1290 UPLC system from same supplier. Compounds were separated in a Zorbax Eclipse Plus C18 rapid resolution column (50 mm × 2.1 mm, 1.8 μm), acquired from Agilent Technologies. Column temperature was set at 40 ºC and the injected volume was 5 μL (15 μL during investigation of TPs and kinetics experiments with unspiked wastewater samples). Ultrapure water (0.1% in FA, phase A) and MeOH (0.1% in FA, phase B) were employed as mobile phases, combined as follows: 2% B (0–2 min), 25% B (8 min), 100% B (15–16 min), 2% B (16.1–21 min). The LC-QTOF-MS instrument was operated in the 2 GHz, extended dynamic resolution mode, with continuous recalibration of the *m/z* axis using the following ions: 121.0508 and 922.0098 (ESI+); 112.9855 and 1033.9881 (ESI-). Typical mass resolution was 17,000 at *m/z* 322.

LC-ESI-TOF-MS records were processed with the MassHunter Qualitative and MassHunter Profinder software packages (Agilent) to identify those molecular features noticed in degradation experiments, which are absent in control assays. The chemical structures of identified TPs were proposed from their product ion spectra, recorded in further injections at different collision energies, considering also the existing background of TRA derivatives reported in previous degradation studies [9,10,15] and using in some photolysis experiments TRA-^{13}C-d_3 as parent compound to confirm the identities of certain TPs.

3. Results and discussion

3.1. Efficiency of oxidative treatments

The efficiency of different treatments for the removal of TRA in model solutions (ultrapure water adjusted at pH 7) was assessed with half-lives values ($t_{1/2}$, min) and observed reaction rate constants (k_{obs}, min^{-1}). In this study, the initial concentrations of oxidants (H_2O_2 or free chlorine) and TRA added to water solutions were 1 mg L^{-1} and 0.005 mg L^{-1}, respectively. TRA remained stable for more than 30 min when exposed to H_2O_2 under above conditions. As regards the rest of treatments, its stability decreased in the following order: free chlorine, UV irradiation, UV-H_2O_2 and UV-chlorine. In all cases, the time-course of TRA fitted a pseudo-first order kinetics model, with determination coefficients (R^2) above 0.98 for the natural logarithmic plots of normalized concentrations versus reaction time. Table 1 summarizes $t_{1/2}$, k_{obs} and R^2 values for each treatment.

During AOPs, k_{obs} values (k_{obsTRA}) reflect the sum of 1st order reaction rate constants of TRA with an excess of the considered oxidant

Table 2
Summary of transformation products generated from TRA noticed using UPLC-QTOF-MS.

Code	Tr (min)	Empirical formula [M+H]+	Experimental *m/z*	Calculated *m/z*	UV	Chlorine	UV-H_2O_2	UV-chlorine	Experimental *m/z* of product ions
TRA	6.25	$C_{16}H_{26}NO_2$	264.1967	264.1964					58.0655
TP142	1.15	$C_8H_{16}NO$	142.1225	142.1232		X	X	X	97.9687; 44.0497
TP156	1.26	$C_9H_{18}NO$	156.1377	156.1383	X		X	X	84.0658; 58.0652
TP170	4.75	$C_9H_{15}NO_2$	170.1173	170.1176				X	142.1226; 111.0802; 72.0448; 60.0444
TP172	1.40	$C_9H_{17}NO_2$	172.1329	172.1332				X	154.1226; 110.0964; 126.1277; 110.0964; 58.0651
TP206	2.08	$C_9H_{16}ClNO_2$	206.0943	206.0942				X	170.1174; 110.0960;92.0254; 84.0808; 58.0652
TP250a	3.93	$C_{15}H_{24}NO_2$	250.1783	250.1802	X		X		58.0652
TP250b	6.45	$C_{15}H_{24}NO_2$	250.1783	250.1802	X	X	X	X	232.1701; 201.1275; 189.1275; 159.0809; 147.0804; 121.0646; 81.0698
TP278	10.78	$C_{16}H_{24}NO_3$	278.1751	278.1756			X	X	201.1275; 159.0804; 121.0648; 72.0444
TP280a	6.63	$C_{16}H_{26}NO_3$	280.1907	280.1913				X	262.798; 201.1269; 135.0436; 121.0650; 58.0653
TP280b	3.50	$C_{16}H_{26}NO_3$	280.1904	280.1913	X		X		248.2447; 135.1161; 58.0652
TP280c	4.94	$C1_6H_{26}NO_3$	280.1546	280.1913	X		X		262.1432; 58.0653
TP280d	5.68	$C_{16}H_{26}NO_3$	280.1901	280.1913	X		X		262.1805; 217.1227; 58.0652
TP296a, d	3.03, 4.78	$C_{16}H_{26}NO_4$	296.1849	296.1862	X		X		58.0653
TP296b, c	4.02, 4.24	$C_{16}H_{26}NO_4$	296.1852	296.1862	X		X		114.0909; 58.0653
TP312a, b	2.12; 3.60	$C_{16}H_{26}NO_5$	312.1801	312.1811	X		X		58.0652
TP346a	2.53	$C_{16}H_{25}ClNO_5$	346.1410	346.1416				X	74.0600; 58.0652
TP346b	2.83	$C_{16}H_{25}ClNO_5$	346.1409	346.1416				X	310.1641; 58.0651
TP350a, b	1.80; 2.20	$C_{15}H_{22}Cl_2NO_4$	350.0921	350.092				X	314.1146; 296.1043; 270.1231; 252.1144; 216.1371; 173.0953; 92.0257; 74.0599; 58.0652; 44.0499
TP394a, b	2.65; 3.87	$C_{16}H_{22}Cl_2NO6$	394.0815	394.0819				X	344.0887; 314.1137; 299.092; 282.0895; 256.0734; 154.1224; 92.0257; 74.0598; 58.0653; 44.0499
TP396	3.33	$C_{16}H_{24}Cl_2NO_6$	396.0973	396.0975				X	378.0861; 58.0656

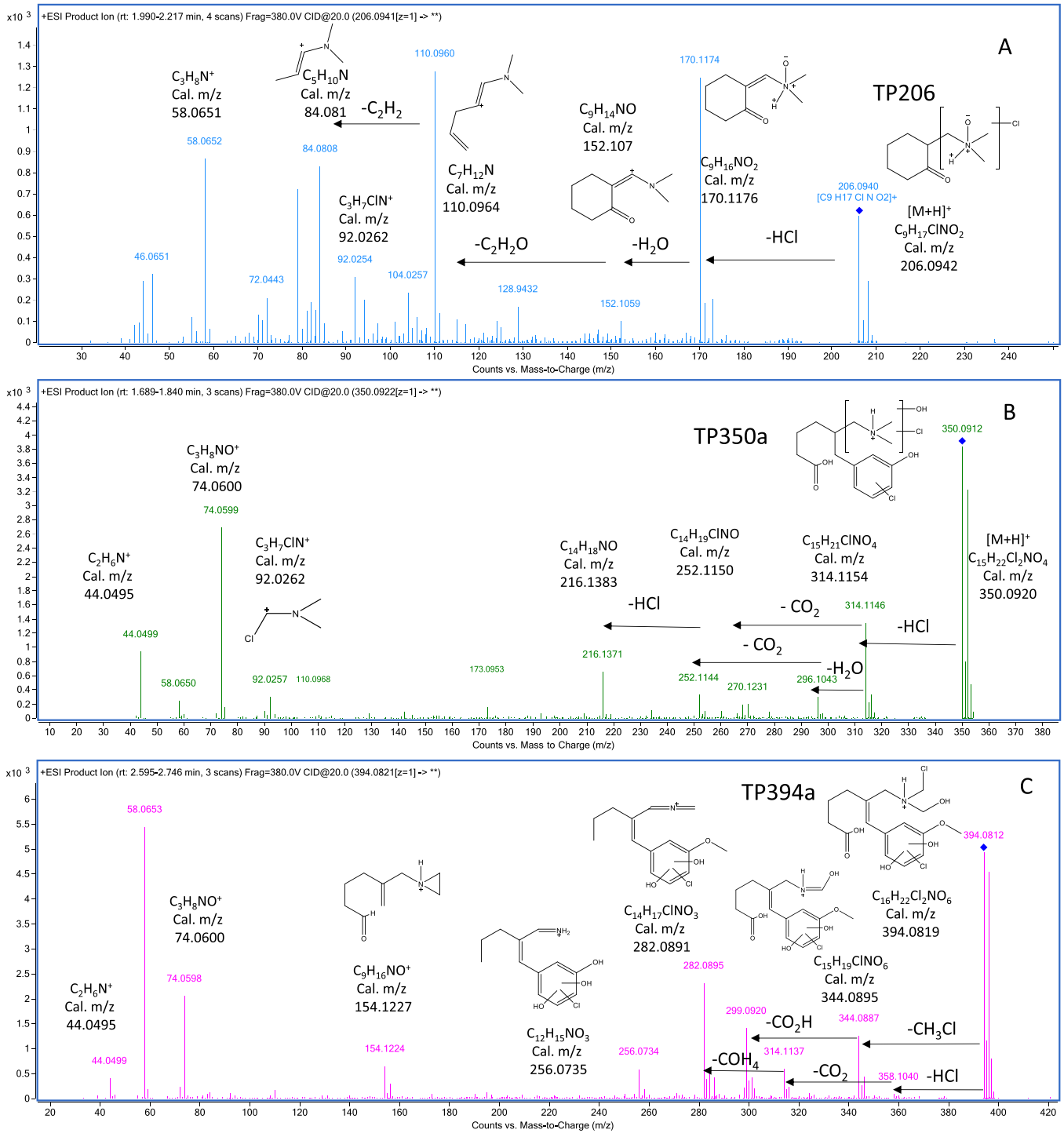

Fig. 1. Product ion spectra and chemical structures assigned to TRA transformation products TP206 (A), TP350a (B) and TP394a (C).

($k_{TRA\text{-}chlorine}$ or $k_{TRA\text{-}H2O2}$), UV light ($K_{TRA\text{-}UV}$) and 2nd order reaction rate with radical species generated during photodecomposition of the employed oxidant: $HO^{\cdot}$ in UV-H_2O_2, and $HO^{\cdot}$ and RCS in UV-chlorine processes. The reaction rate of TRA with $HO^{\cdot}$ ($k_{TRA\text{-}HO}$) was evaluated following a competitive kinetics experiment in presence of CBA. The assay was carried out as reported elsewhere [22], using 1 mM as the initial concentrations of H_2O_2, and 5 μM for TRA and CBA. Both compounds remained stable in contact with H_2O_2 (1 mM); thus, their observed reaction rate constants ($k_{obsCBA(TRA)\text{-}UV\text{-}H2O2}$ and $k_{obsTRA(CBA)\text{-}UV\text{-}H2O2}$) can be described using the following expressions (Eqs. (4 and 5)):

$$k_{obsCBA\ (TRA)\text{-}UV\text{-}H2O2} = k_{CBA\text{-}UV} + k'_{CBA\text{-}HO}\,[HO^{\cdot}] \quad (4)$$

$$k_{obsTRA(CBA)\text{-}UV\text{-}H2O2} = k_{TRA\text{-}UV} + k'_{TRA\text{-}HO}\,[HO^{\cdot}] \quad (5)$$

Table S3 summarized the experimental values of the observed reaction rate constants, and the direct photolysis rate constant of CBA ($k_{CBA\text{-}UV}$). Combining these data with the experimental $k_{TRA\text{-}UV}$ (Table 1), and the known value for the second order rate constant of CBA with $HO^{\cdot}$ ($k'_{CBA\text{-}HO}$ 3.0 $\times 10^{11}$ M^{-1} min^{-1}) [22], the calculated value of $k'_{TRA\text{-}HO}$ was 2.69 $\times$ 10^{11} M^{-1} min^{-1}.

Using a similar balance to those described by Eqs. (4 and 5), $k_{obsTRA\text{-}}$

$_{UV\text{-}chlorine}$ can be written as the sum of four contributions (Eq. (6)) [23]. The latter term in Eq. (6) represents the pseudo-first-order reaction rate constant of TRA with RCS species generated in the UV-chlorine treatment.

$$k_{obsTRA\text{-}UV\text{-}chlorine} = k_{TRA\text{-}chlorine} + k_{TRA\text{-}UV} + k_{TRA\text{-}HO}[HO^{\cdot}] + k_{obs,\ RCS} \quad (6)$$

The concentration of $HO^{\cdot}$ radicals generated during the UV-chlorine treatment (using 1 mg L^{-1} of free chlorine, at pH 7) was calculated using NB as model compound. The 2nd order reaction rate of NB with $HO^{\cdot}$ ($K_{NB\text{-}HO}$.) has a value of 2.34×10^{11} $M^{-1}min^{-1}$. NB does not react with RCS [17,22]; moreover, it remained stable in presence of free chlorine levels up to 10 mg L^{-1} (Fig. S1). The experimental values of $k_{NB\text{-}UV}$ and $k_{obsNB\text{-}UV\text{-}chlorine}$ were 0.0016 and 0.041 min^{-1}, respectively, Fig. S1. Introducing these values in Eq. (7), we calculated that the concentration of $HO^{\cdot}$ radicals generated during UV decomposition of 1 mg L^{-1} of chlorine. The obtained value was 1.68×10^{-13} M. Combining this value with data compiled in Table 1, and applying Eq. (6), the $K_{obsTRA\text{-}RCS}$ has a value of 0.2639 min^{-1}. In summary, considering 1 mg L^{-1} as the initial concentration of free chlorine, at a UV light fluence reaching the sample of 1.04×10^{-6} Einstein $L^{-1}s^{-1}$, the relative contributions of chlorination, direct photolysis, $HO^{\cdot}$ radicals and RCS to the degradation of TRA were 5.8%, 12.5%, 12.0% and 69.7%, respectively. As discussed further, in Section 3.3, the importance of RCS during UV/free chlorine dissipation of TRA is in agreement with the identification of chlorinated transformation products, including the formation of chlorinated phenols and chlorination of alkyl chains bonded to the tertiary amine moiety in the molecule of tramadol.

$$k_{obsNB\text{-}UV\text{-}chlorine} = k_{NB\text{-}UV} + k_{NB\text{-}HO}[HO^{\cdot}] \quad (7)$$

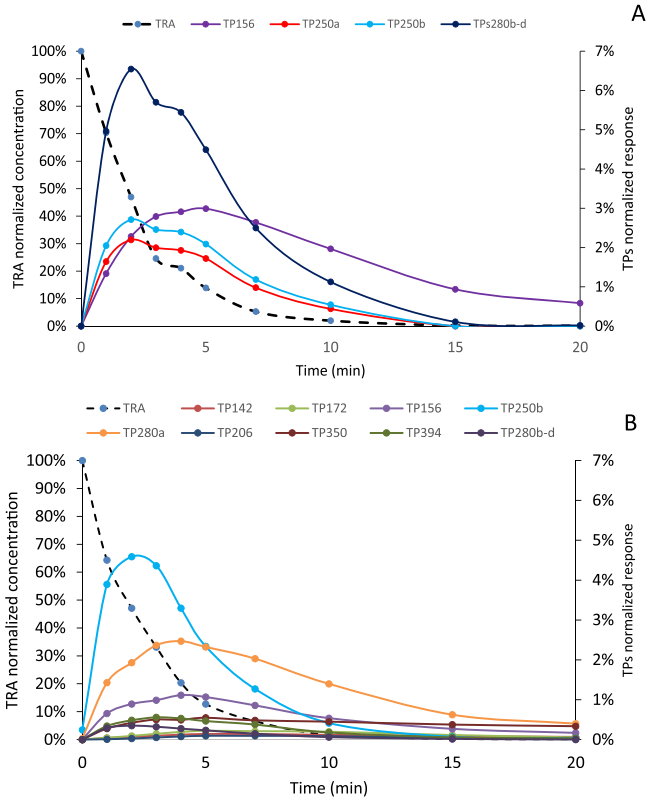

Fig. 2. Evolution of tramadol (left axis) and its main TPs (right axis) in model ultrapure water solutions. A, UV-H_2O_2. B, UV-chlorine.

3.2. Comparative study of transformation products

Table 2 summarizes the list of TPs identified by LC-QTOF-MS during different treatments (UV, chlorine, UV-H_2O_2 and UV-chlorine) applied to ultrapure water solutions, spiked with an initial concentration of TRA of 0.5 mg L^{-1}. Levels of oxidants were 10 mg L^{-1} (chlorine) and 5 mg L^{-1} (H_2O_2), equivalent to a molar concentration of 0.14 mM for both species.

TPs are labeled with a code corresponding to the nominal mass of their protonated molecules ($[M+H]^+$ ion). In addition to retention times and proposed formulae, the *m/z* values of most intense ions in their spectra (product ion) are also included in Table 2. All spectral data were recorded using ESI(+) ionization, since no TPs were noticed under ESI (-). The set of TPs was generated through different reaction routes involving N- and O-desmethylation, N-oxidation, hydroxylation, alkyl oxidation, chlorination, opening of the cyclohexane ring followed by oxidation, and cleavage of the bond between anisole and cyclohexane rings.

UV photolysis led to formation of both desmethylated TRA derivatives (TPs250a and 250b). TP250a was identified as the O-desmethyl species since same compound was formed from TRA and TRA-^{13}C-d_3, whilst TP250b was N-desmethyl TRA (confirmed with a commercial standard). TP156 was generated through hydrolysis of the bond connecting cyclohexane and anisole rings in the molecule of TRA. The three species have been previously reported as TPs of TRA. Their spectra are given in Fig. S2. Several hydroxylated derivatives containing one (TPs280b to 280d), two (TPs296a to 296d), or three hydroxyl moieties (TPs 312a and 312b) were also noticed during UV irradiation of TRA spiked water samples. The spectra of these hydroxylated TPs (Fig. S2) match those assigned to derivatives described during photocatalytic degradation of TRA in presence of TiO_2 [15]. However, the exact position of hydroxyl groups could not be identified since major MS/MS transitions reflected just the removal of H_2O from their $[M+H]^+$ ions, and a common fragment for the trimethyl amino ion ($[C_3H_8N]^+$, calculated *m/z* 58.0654).

Free chlorine led to formation of N-desmethyl TRA (TP250b) and its secondary hydrolysis derivative (TP142). Under employed conditions (samples buffered at pH 7, 10 mg L^{-1} of chlorine), we did not detect the formation of chlorinated species previously reported using higher chlorine doses, and samples buffered at pH values in the range from 4 to 9 units [9].

Combination of UV and H_2O_2 turned in similar TPs to those noticed under direct photolysis in addition to a carbonyl derivative of TRA (TP278) and TP142, Table 2. Regarding TP278, its product ion spectra (Fig. S2) did not permit to discriminate whether it corresponds to an aldehyde (resulting from oxidation of one of the primary carbons bonded to the atom of nitrogen) or to a ketone (oxidation in the secondary carbon). The aldehyde structure was described during free chlorine treatment of TRA spiked waters [9]; whilst formation of a ketone has been reported from the pharmaceutical venlafaxine, which shares the same tertiary amine group as TRA [24].

UV-chlorine treatment rendered the highest number of TPs. Among them, TPs 142, 156 and 170 are secondary hydrolysis derivatives of TP250b, TRA and TP278, respectively. TP280a was confirmed as the N-oxide of TRA, which has been previously reported during ozonization processes carried out at pilot scale [14]. TPs 172 and 206 are also specific for the UV-chlorine treatment. TP172 results from hydrolysis of TP280a, and TP206 is a chlorinated derivative of TP172. This assumption was confirmed with further UV-chlorine experiments using water samples spiked with a commercial standard of TRA N-oxide (TP280a). The spectra of TP206 contains a weak cluster of ions at *m/z* 92.0253, Fig. 1 A. The empirical formula assigned to this ion ($[C_3H_7ClN]^+$) suggests that TP206 is chlorinated in any of the carbons in alpha position to the atom of nitrogen. The O-desmethyl derivative of TRA (TP250a) was not observed during UV-chlorine treatment. We assume that this phenolic intermediate undergoes further, fast hydroxylation and/or chlorination reactions. This way, TPs350a and 350b might arise from

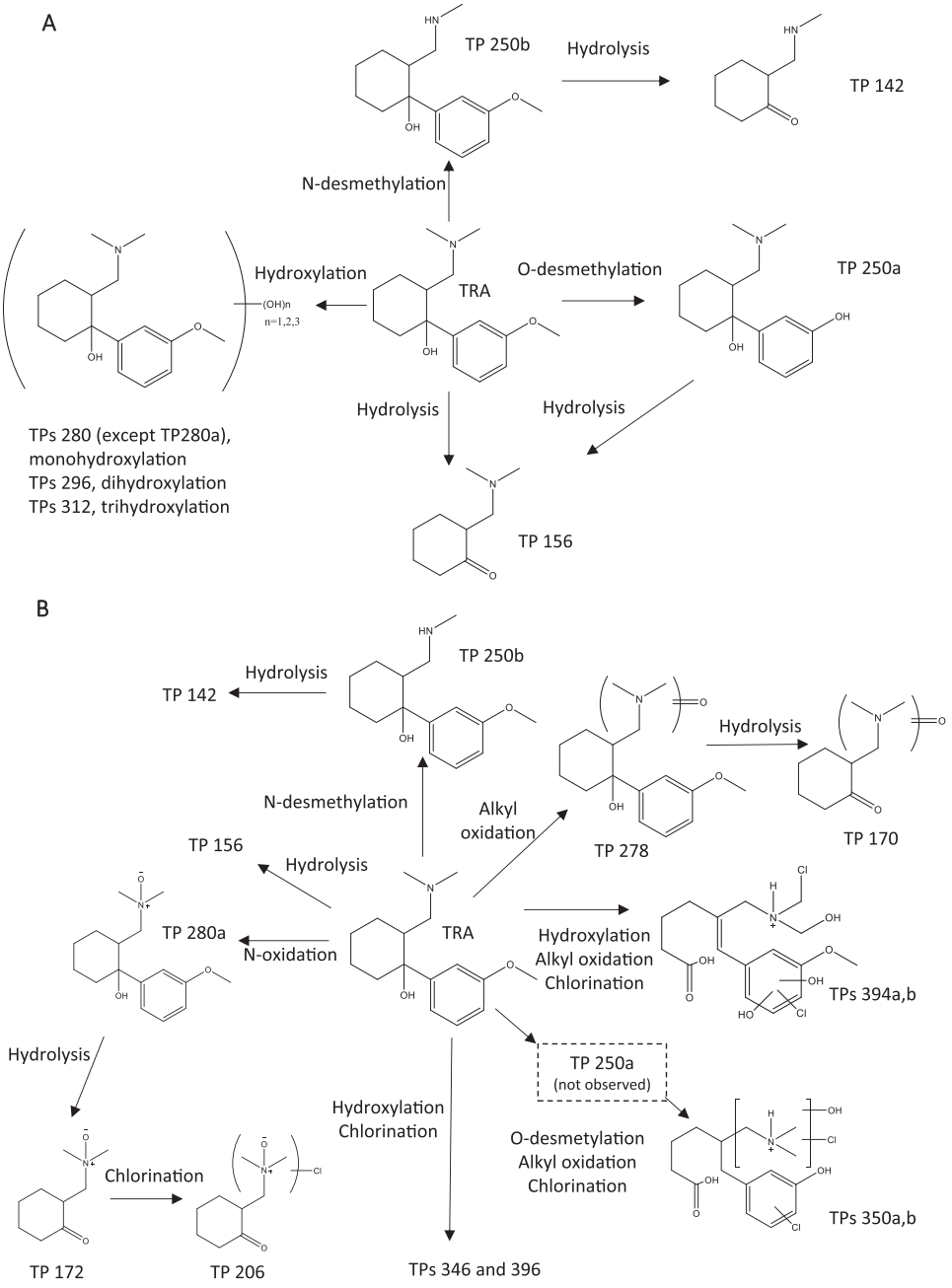

Fig. 3. Reaction routes of TRA in UV-H_2O_2 (A) and UV-chlorine (B) AOPs.

this intermediate. This assumption is made considering the electrophilic behavior of $HO^{\cdot}$ and $Cl^{\cdot}$ radicals, and the strong activation effect of the phenolic group to electrophilic substitution reactions [17,24]. Both, TPs350a and 350b presented the same spectra. Fig. 1B shows one of these spectra and a tentative structure of the TP. Again, the spectrum contains a weak product ion at *m/z* 92.0261, assigned to fragment ion $[C_3H_7ClN]^+$; moreover, some of the experimental transitions (314.1146 > 270.1231, 296.1043 > 252.1144) correspond to the removal of CO_2. Likely, formation of this compound involves hydroxylation of the aliphatic cycle followed by ring opening and further oxidation to a carboxylic acid. Likely, the second atom of chlorine is attached to the aromatic ring in ortho or para positions to the phenolic group, which explains the existence of two isomers.

TPs 394a and 394b are also dichloro derivatives of TRA, maintaining the same number of carbons as the parent compound and incorporating one additional unsaturation. The tentative structure assigned to these compounds and the spectrum of TP 394a are shown in Fig. 1 C. The observed transitions are compatible with chlorination in a terminal carbon (394.0812 > 344.0887) and CO_2 removal (358.1040 > 314.1137). TPs 394a and 394b are considered positional isomers, with two hydroxyls and one atom of chlorine attached to the anisole ring, whilst a third hydroxyl and another chlorine are in alpha to the tertiary amine group. The aliphatic part of the molecule includes a C-C double bond and a carboxylic group formed after opening of the cyclohexane ring.

Finally, spectra of TPs346a, 346b and 396 (mono and di-chlorinated species) do not contain useful information to identify positions of hydroxyl and chlorine substituents, Fig. S2. According to their empirical formulae, TPs346a and 346b are mono-chlorinated derivatives of a trihydroxylated form of TRA, and TP396 is a di-chlorinated and tetrahydroxylated derivative of TRA.

Fig. 2 shows the time-course of TRA and its TPs during UV-H_2O_2

(Fig. 2 A) and UV-chlorine (Fig. 2B) treatments, respectively. In the second case, data for TP346 and TP396 have not been included in the figure. Their maximum responses hardly represented 0.05% of that obtained for TRA at zero time. Whatever the water treatment, after 20 min, most of the TPs were either not detected, or their relative response represented less than 0.5% of that obtained for TRA at zero time. Therefore, TPs included in Fig. 2 are amenable to further degradation. In case of TPs 250b and 280a (N-desmethyl TRA and TRA-N-oxide, respectively), the responses provided by the LC-ESI-TOF-MS system for their $[M+H]^+$ ions were similar to that obtained for TRA; thus, normalized responses can be associated to normalized concentrations. Consequently, even though TP280a is known to have a higher toxicity than TRA, less than 0.5% of the initial TRA remains as TRA N-oxide after 20 min of treatment, Fig. 2B. The maximum yield of TPs 250b and 280a formation from TRA observed in this research was similar to that reported during photocatalytic treatment in presence of TiO_2 [15]; however, using UV-chlorine, the highest conversion rate was noticed at shorter irradiation times followed by steady decrease in the levels of both TPs.

During above AOPs, the concentration of H_2O_2 was checked to remain stable during 20 min (data not shown); whilst in case of UV-free chlorine, the level of oxidant decreased slowly, but steady with reaction time to 70% of its initial value after 20 min, see Fig. S3A. The TOC of reaction mixtures under UV/H_2O_2 and UV/free chlorine treatments are also provided as supplementary information, Fig. S3B. Data are shown as normalized values to the concentration measured at zero time. For the UV/H_2O_2 treatment, the content of organic carbon remained unchanged during the process; thus, mineralization is excluded. In case of UV/free chlorine, a reduction of TOC was appreciated after 10 min, despite the final value obtained after 20 min still represented 80% of that existing in the solution at the beginning of the experiment. Thus, additional compounds to those summarized in Table 2 (likely small molecules not amenable to LC-ESI-QTOF-MS determination) remain in the water solution.

The time-course profiles of TPs observed using direct photolysis and free chlorine alone are provided as supplementary information, Fig. S4. Major TPs noticed after 30 min were TP156 and TP250b for UV and free chlorine treatments, respectively. Their relative responses represented up to 20% of that of TRA in the zero time aliquot.

Regarding volatile species, after 20 min of UV-chlorine treatment of model solutions spiked with 0.5 mg L^{-1} and 10 mg L^{-1} of TRA and free chlorine, formation of chloroform, 1,1-dichloroacetone and anisole was noticed using LLE followed by GC-TOF-MS. Measured concentrations were in the range of 0.001–0.002 mg L^{-1} for the chlorinated compounds and 0.007 mg L^{-1} of anisole, respectively. These values represent between 0.2% and 1.4% of the concentration of TRA added to the aqueous solution.

Considering the spectral data of TPs, and the identities (confirmed or tentative) assigned to these compounds, the different routes observed during UV-H_2O_2 and UV-chlorine treatment of TRA spiked model aqueous solutions, buffered at pH 7, are shown in Fig. 3. Although UV-chlorine was the most effective treatment, it increased the potential reaction routes of TRA, leading to formation of several chlorinated species, some of them reported for the first time in this research.

3.3. Effect of inorganic species on UV-H_2O_2 and UV-chlorine kinetics

Anionic species, existing in environmental water samples, are scavengers of radicals generated in AOPs, reducing their efficiency. Particularly, bicarbonate (the major source of inorganic carbon in neutral pH waters) consumes $HO^{\cdot}$ and $Cl^{\cdot}$ species (Eqs. (8 and 9)) leading to formation of the carbonate radical, with a lower redox potential than precursor species [17,25].

$$HO^{\cdot} + HCO_3^- \rightarrow H_2O + CO_3^{\cdot-},\ k = 8{\cdot}5\times10^6\ M^{-1}s^{-1} \quad (8)$$

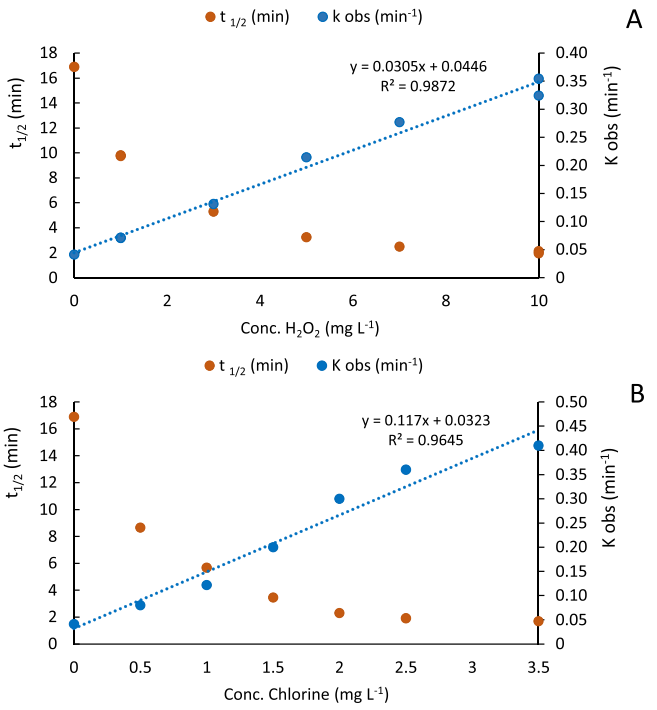

Fig. 4. Half-lives ($t_{1/2}$, min) and observed reaction rate constant (K_{obs}, min^{-1}) of TRA in spiked river water, pH 7, as function of the type and the concentration of oxidant. A, UV-H_2O_2. B, UV-chlorine.

$$Cl^{\cdot} + HCO_3^- \rightarrow HCl + CO_3^{\cdot-},\ k = 2{\cdot}2\times10^8\ M^{-1}s^{-1} \quad (9)$$

Chlorides and nitrates, participate in similar quenching reactions reducing the available amounts of $HO^{\cdot}$ and $Cl^{\cdot}$. On the other hand, ammonium combines with free chlorine producing chloramines; thus, it is expected to reduce the efficiency of UV-chlorine combined treatments [26]. The relative variations in the $t_{1/2}$ of TRA during UV-H_2O_2 and UV-chlorine processes (pH 7, using 1 mg L^{-1} as initial concentration of oxidant), in presence of the above species, versus values observed in model ultrapure water solutions are shown in Fig. S5. The added concentrations of ammonium, chloride or nitrate (1, 70 and 50 mg L^{-1}, respectively) were similar to their usual, or maximum values in treated wastewater and surface water (nitrates). The level of bicarbonate (200 mg L^{-1}) was twice higher than the equivalent inorganic carbon existing in further considered wastewater samples, Table S2. Bicarbonate showed a similar negative influence on the degradability of TRA under both AOPs. Efficiency of UV-H_2O_2 treatment was more sensitive to chlorides and nitrates than that of UV-chlorine. Finally, the negative impact of ammonium was significantly higher in case of UV-chlorine, Fig. S5.

3.4. Degradation efficiency in environmental water samples

The efficiencies of UV-chlorine and UV-H_2O_2 were re-evaluated with three environmental water matrices, corresponding to river water (spiked with TRA at 0.005 mg L^{-1}) and two samples of treated wastewater (TRA contents of 0.0019 mg L^{-1} and 0.0020 mg L^{-1}, samples code A and B, respectively) using different doses of the considered oxidant. The content in different anions in these samples, their total dissolved carbon, organic carbon and absorbance at 254 nm are given in Table S2. Fig. 4 shows the k_{obs} and $t_{1/2}$ of TRA in the river water matrix. The values of $k_{obsUV\text{-}H2O2}$ increased linearly with the concentration of oxidant in the range from 0 to 10 mg L^{-1}, Fig. 4 A. The $k_{obsUV\text{-}chlorine}$ increased also with the level of chlorine; however, no additional improvement was noticed for values above 3.5 mg L^{-1}, Fig. 4B. This finding suggests that the auto-quenching effects of radical species, by reaction with the excess of oxidant, were more relevant for the UV-

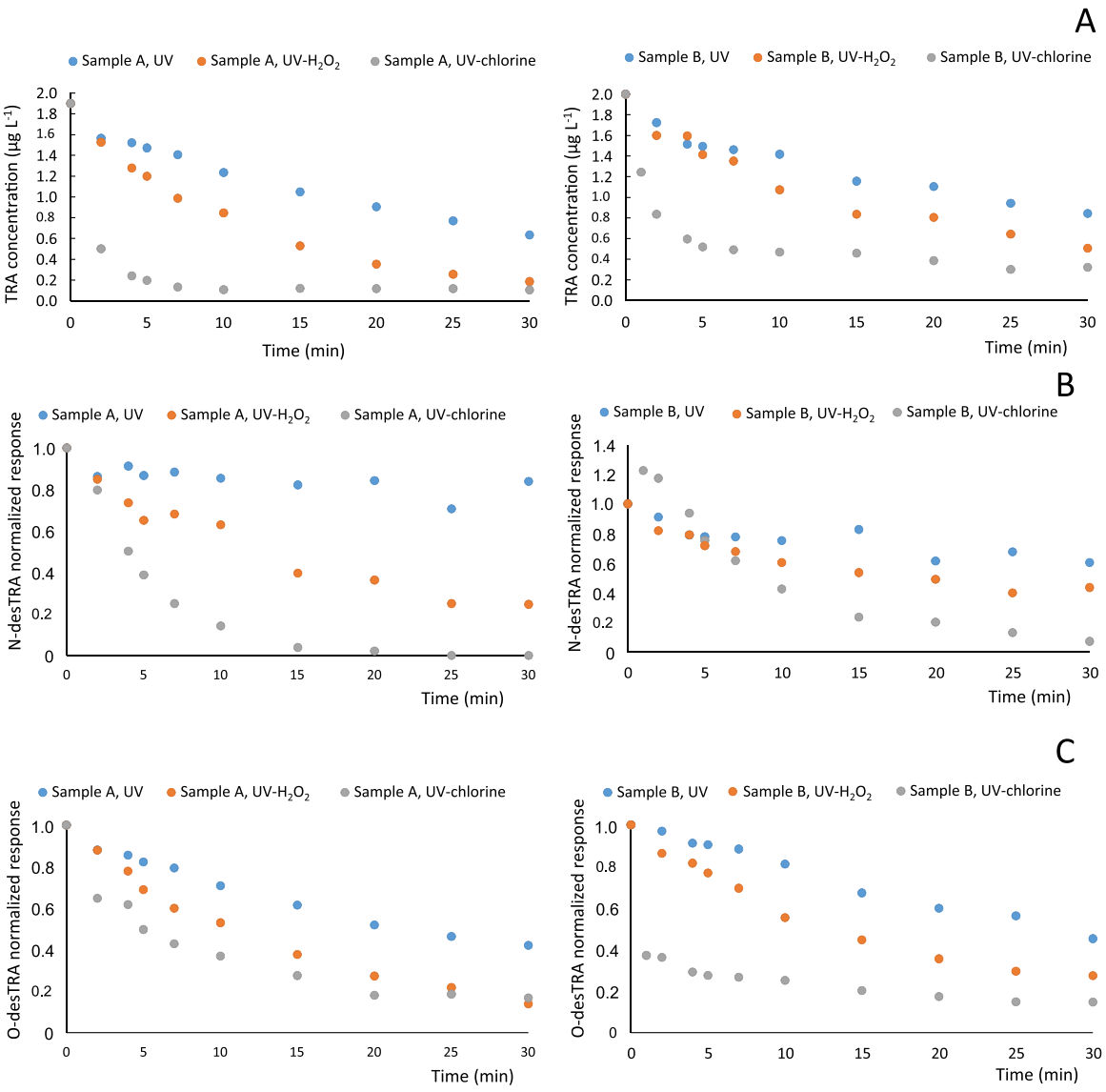

Fig. 5. Time-course plots of TRA concentrations (A), and N-desmethyl TRA (B) and O-desmethyl TRA (C) normalized responses in two non-spiked wastewater samples (left, sample code A; right, sample code B) under UV, UV-H_2O_2 and UV-chlorine treatments. Data for samples buffered at pH 7, using 10 mg L^{-1} as initial concentration of the selected oxidant.

chlorine system than for UV-H_2O_2 [16]. Under conditions considered in Fig. 4, the degradation of TRA fitted a first-order model; however, 3-times higher concentrations of oxidants were required to achieve similar $t_{1/2}$ values to those reported in Table 1 for model ultrapure water solutions.

Fig. 5 A shows the time-course of TRA concentrations in two unspiked wastewaters (left sample A, right sample B), buffered at pH 7, under direct photolysis, UV- H_2O_2, and UV-chlorine. Depicted data correspond to an initial concentration of oxidants of 10 mg L^{-1}. Using doses below 5 mg L^{-1}, no differences were noticed between the efficiency of UV irradiation and the two AOPs, data not shown. Whatever the tested treatment, for wastewater code A (showing the lower absorbance at 254 nm, Table S2), TRA was removed in a higher extent than in case of wastewater code B, Fig. 5 A. In both samples, the efficiency of the treatment increased following the same pattern as in ultrapure model solutions: UV < UV-H_2O_2 < UV-chlorine. The rate of TRA degradation using UV and UV-H_2O_2 fitted a first-order kinetics model; however, in the case of UV-chlorine, the degradation rate decreased significantly after 5 min. The photometric determination of available free chlorine showed levels of only 6 mg L^{-1}, at reaction times of 5 min, which further decreased to 1.3 mg L^{-1} at 15 min (data not shown); so, the reduction of tramadol dissipation rate observed in Fig. 5 (particularly for sample B) was in agreement with the fast consumption of free chlorine in wastewater samples. Despite this reduction, for irradiation times below 30 min, UV-chlorine demonstrated a higher efficiency than UV-H_2O_2. The difference in efficiencies is more evident at shorter reaction times (i.e. 5 min).

Regarding TPs compiled in Table 2, their formation was not observed during treatment of non-spiked wastewater samples. Assuming similar LOQs for these compounds to that obtained for TRA (0.04 µg L^{-1}), considering the initial concentration of TRA in the wastewater samples (ca. 2 µg L^{-1}) and transformation percentages shown in Fig. 2B, this was an expected result. For TP280a (TRA-N-oxide), the combination of a large volume injection method (0.1 mL) with a LC-QqQ-MS instrument, permitted to state that this TPs was not generated at concentrations above 0.002 µg L^{-1}. Formation of the desmethyl forms of TRA (TPs 250a and 250b) was most difficult to identify, since both compounds occurred in the wastewater samples. Their evolution during above treatments is shown in Fig. 5B (N-desmethyl TRA, TP250b) and Fig. 5 C (O-desmethyl TRA, TP250a). Their time-course profiles demonstrated again the higher

efficiency of UV-chlorine versus direct photolysis and UV-H_2O_2 to remove these active metabolites from wastewater samples. Again, faster dissipation was noticed in wastewater code A (left graphs) than in sample code B (right graphs). In case of N-desmethyl TRA (TP250b), an initial increase in the response of this compound was noticed during the first 2 min, in one of the wastewater samples (Fig. 5B, right), followed by a steady reduction. After 30 min of UV-chlorine treatment, the levels of N and O-desmethyl TRA existing in both wastewater samples were reduced in more than 80%.

4. Conclusions

At neutral pH values, the combination of UV with free chlorine was the most effective of the tested processes for the removal of TRA from spiked model solutions, surface and non-spiked wastewater samples previously submitted to a biological treatment. Shorter half-lives and higher observed reaction rate constants for UV-chlorine are coherent with the significant contribution of RCS to TRA degradation, the higher molar absorptivity of free chlorine compared to hydrogen peroxide, and the identification of specific reaction routes for UV-chlorine process not observed during UV-H_2O_2. Despite the fact that some of the TPs observed during UV-chlorine have been described as more concerning than the parent compound, i.e. TRA-N-oxide, maximum conversion rates found in this study remained below 3%. Regarding chlorinated derivatives (non-volatile and volatile ones) and other transformation products identified by GC-TOF-MS, their levels (concentrations in case of chloroform, 1,1-dichloroacetone and anisole) represented less than 2% of that measured for TRA in the non-treated samples. For the most complex of the water matrices considered in this research, a concentration of 10 mg L^{-1} of chlorine combined with UV irradiation, achieved a dramatic reduction in the levels of TRA, and its two human metabolites, found in wastewater samples, despite the rate of tramadol removal decreased significantly after 5 min. Further research is required to (1) correlate the composition of environmental water samples with the minimum concentration of oxidant required to enhance the efficiency of UV-chlorine versus direct photolysis, (2) scale-up and confirm the efficiency of UV-free chlorine at pilot plant level, and (3) using in-vitro studies to follow the time-course toxicity of complex reaction mixtures generated during UV/free chlorine treatment.

CRediT authorship contribution statement

M. Cobo: Investigation, Methodology, Writing – original draft. **V. Fernández**: Investigation, Methodology. **T. Arias**: Investigation. **M. Ramil**: Data curation, Formal analysis, Writing – review & editing. **R. Cela**: Project administration, Funding acquisition, Writing – review & editing. **I. Rodríguez**: Conceptualization, Supervision, Funding acquisition, Writing – original draft.

Declaration of Competing Interest

The authors declare that they have no known competing financial interests or personal relationships that could have appeared to influence the work reported in this paper.

Acknowledgements

This study was supported through grants PGC2018-094613-B-I00 and ED431C 2021/06, funded by Spanish Government (Ministry of Science, Innovation and Universities) and Xunta de Galicia, respectively. Both projects are co-funded by the EU FEDER program. M.C.G. thanks a FPI fellowship to the Ministry of Science and Education (Spain).

Appendix A. Supporting information

Supplementary data associated with this article can be found in the online version at doi:10.1016/j.jece.2022.107854.

References

[1] T. Boogaerts, M. Quireyns, A. Covaci, H. De Loof, A.L.N. van Nuijs, Analytical method for the simultaneous determination of a broad range of opioids in influent wastewater: optimization, validation and applicability to monitor consumption patterns, Talanta 232 (2021), 122443, https://doi.org/10.1016/j.talanta.2021.122443.
[2] K.S. Hakala, R. Kostiainen, R.A. Ketola, Feasibility of different mass spectrometric techniques and programs for automated metabolite profiling of tramadol in human urine, Rapid Commun. Mass Spectrom. 20 (2006) 2081–2090, https://doi.org/10.1002/rcm.2562.
[3] R. Gurke, M. Rößler, C. Marx, S. Diamond, S. Schubert, R. Oertel, J. Fauler, Occurrence and removal of frequently prescribed pharmaceuticals and corresponding metabolites in wastewater of a sewage treatment plant, Sci. Total Environ. 532 (2015) 762–770, https://doi.org/10.1016/j.scitotenv.2015.06.067.
[4] N. Hermes, K.S. Jewell, M. Schulz, J. Müller, U. Hübner, A. Wick, J.E. Drewes, T. A. Ternes, Elucidation of removal processes in sequential biofiltration (SBF) and soil aquifer treatment (SAT) by analysis of a broad range of trace organic chemicals (TOrCs) and their transformation products (TPs), Water Res. 163 (2019), 114857, https://doi.org/10.1016/j.watres.2019.114857.
[5] P. Verlicchi, M. Al Aukidy, E. Zambello, Occurrence of pharmaceutical compounds in urban wastewater: removal, mass load and environmental risk after a secondary treatment-a review, Sci. Total Environ. 429 (2012) 123–155, https://doi.org/10.1016/j.scitotenv.2012.04.028.
[6] B. Kasprzyk-Hordern, R.M. Dinsdale, A.J. Guwy, The removal of pharmaceuticals, personal care products, endocrine disruptors and illicit drugs during wastewater treatment and its impact on the quality of receiving waters, Water Res. 43 (2009) 363–380, https://doi.org/10.1016/j.watres.2008.10.047.
[7] D. Sadutto, V. Andreu, T. Ilo, J. Akkanen, Y. Picó, Pharmaceuticals and personal care products in a Mediterranean coastal wetland: impact of anthropogenic and spatial factors and environmental risk assessment, Environ. Pollut. 271 (2021), https://doi.org/10.1016/j.envpol.2020.116353.
[8] A.C. Kondor, G. Jakab, A. Vancsik, T. Filep, J. Szeberényi, L. Szabó, G. Maász, Á. Ferincz, P. Dobosy, Z. Szalai, Occurrence of pharmaceuticals in the danube and drinking water wells: efficiency of riverbank filtration, Environ. Pollut. 265 (2020), https://doi.org/10.1016/j.envpol.2020.114893.
[9] H. Cheng, D. Song, Y. Chang, H. Liu, J. Qu, Chlorination of tramadol: reaction kinetics, mechanism and genotoxicity evaluation, Chemosphere 141 (2015) 282–289, https://doi.org/10.1016/j.chemosphere.2015.06.034.
[10] J. Radjenovic, M.J. Farré, W. Gernjak, Effect of UV and UV/H2O2 in the presence of chloramines on NDMA formation potential of tramadol, Environ. Sci. Technol. 46 (2012) 8356–8364, https://doi.org/10.1021/es301625k.
[11] K.M. Blum, S.H. Norström, O. Golovko, R. Grabic, J.D. Järhult, O. Koba, H. Söderström Lindström, Removal of 30 active pharmaceutical ingredients in surface water under long-term artificial UV irradiation, Chemosphere 176 (2017) 175–182, https://doi.org/10.1016/j.chemosphere.2017.02.063.
[12] D.B. Miklos, R. Hartl, P. Michel, K.G. Linden, J.E. Drewes, U. Hübner, UV/H2O2 process stability and pilot-scale validation for trace organic chemical removal from wastewater treatment plant effluents, Water Res. 136 (2018) 169–179, https://doi.org/10.1016/j.watres.2018.02.044.
[13] B.A. Wols, C.H.M. Hofman-Caris, D.J.H. Harmsen, E.F. Beerendonk, Degradation of 40 selected pharmaceuticals by UV/H2O2, Water Res. 47 (2013) 5876–5888, https://doi.org/10.1016/j.watres.2013.07.008.
[14] S. Kharel, M. Stapf, U. Miehe, M. Ekblad, M. Cimbritz, P. Falås, J. Nilsson, R. Sehlén, K. Bester, Ozone dose dependent formation and removal of ozonation products of pharmaceuticals in pilot and full-scale municipal wastewater treatment plants, Sci. Total Environ. 731 (2020), https://doi.org/10.1016/j.scitotenv.2020.139064.
[15] M. Antonopoulou, I. Konstantinou, Photocatalytic degradation and mineralization of tramadol pharmaceutical in aqueous TiO2 suspensions: evaluation of kinetics, mechanisms and ecotoxicity, Appl. Catal. A Gen. 515 (2016) 136–143, https://doi.org/10.1016/j.apcata.2016.02.005.
[16] G. Castro, M. Ramil, R. Cela, I. Rodríguez, Assessment of UV combined with free chlorine for removal of valsartan acid from water samples, Sci. Total Environ. 762 (2021), 143173, https://doi.org/10.1016/j.scitotenv.2020.143173.
[17] N. Kishimoto, State of the art of UV/chlorine advanced oxidation processes: their mechanism, byproducts formation, process variation, and applications, J. Water Environ. Technol. 17 (2019) 302–335, https://doi.org/10.2965/jwet.19-021.
[18] X. Kong, J. Jiang, J. Ma, Y. Yang, W. Liu, Y. Liu, Degradation of atrazine by UV/chlorine: efficiency, influencing factors, and products, Water Res. 90 (2016) 15–23, https://doi.org/10.1016/j.watres.2015.11.068.
[19] M. Simmons George, Standard methods for the examination of water and waste water, J. N. Am. Benthol. Soc. 12 (1993) 308–309, https://doi.org/10.2307/1467470.
[20] I. Carpinteiro, G. Castro, I. Rodríguez, R. Cela, Free chlorine reactions of angiotensin II receptor antagonists: kinetics study, transformation products elucidation and in-silico ecotoxicity assessment, Sci. Total Environ. 647 (2019) 1000–1010, https://doi.org/10.1016/j.scitotenv.2018.08.082.
[21] D.P. Hautman, D.J. Munch, Development of U.S. EPA Method 551.1, J. Chromatogr. Sci. 35 (1997) 221–231, https://doi.org/10.1093/chromsci/35.5.221.
[22] Y. Yang, J. Jiang, X. Lu, J. Ma, Y. Liu, Production of sulfate radical and hydroxyl radical by reaction of ozone with peroxymonosulfate: a novel advanced oxidation

process, Environ. Sci. Technol. 49 (2015) 73307339, https://doi.org/10.1021/es506362e.
[23] Q. Li, C. Lai, J. Yu, J. Luo, J. Deng, G. Li, W. Chen, B. Li, G. Chen, Degradation of diclofenac sodium by the UV/chlorine process: reaction mechanism, influencing factors and toxicity evaluation, J. Photochem. Photobiol. A Chem. 425 (2022), 113667, https://doi.org/10.1016/j.jphotochem.2021.113667.
[24] T. Zhu, J. Deng, S. Zhu, A. Cai, C. Ye, X. Ling, H. Guo, Q. Wang, X. Li, Kinetic and mechanism insights into the degradation of venlafaxine by UV/chlorine process: a modelling study, Chem. Eng. J. 431 (2022), 133473, https://doi.org/10.1016/j.cej.2021.133473.
[25] B. Nikravesh, A. Shomalnasab, A. Nayyer, N. Aghababaei, R. Zarebi, F. Ghanbari, UV/Chlorine process for dye degradation in aqueous solution: mechanism, affecting factors and toxicity evaluation for textile wastewater, J. Environ. Chem. Eng. 8 (2020), https://doi.org/10.1016/j.jece.2020.104244.
[26] E. Rott, B. Kuch, C. Lange, P. Richter, R. Minke, Influence of ammonium ions, organic load and flow rate on the UV/chlorine AOP applied to effluent of a wastewater treatment plant at pilot scale, Int. J. Environ. Res. Public Health 15 (2018), https://doi.org/10.3390/ijerph15061276.